

## Geochemistry, Geophysics, Geosystems

### RESEARCH ARTICLE

10.1029/2018GC007474

#### Key Points:

- Systematic investigations of seismic anisotropy beneath the Indochina Peninsula were conducted using data from a total of 29 stations
- E-W fast orientations at most stations in central and northern Peninsula are attributed to flow from plate motion or slab rollback
- Mantle upwelling is responsible for weak anisotropy with non-E-W fast orientations at stations in the southern 1/3 of the Peninsula

#### Supporting Information:

- Table S1

#### Correspondence to:

Y. Yu,  
yuyouqiang@tongji.edu.cn

#### Citation:

Yu, Y., Gao, S. S., Liu, K. H., Yang, T., Xue, M., Le, K. P., & Gao, J. (2018). Characteristics of the mantle flow system beneath the Indochina Peninsula revealed by teleseismic shear wave splitting analysis. *Geochemistry, Geophysics, Geosystems*, 19, 1519–1532. <https://doi.org/10.1029/2018GC007474>

Received 2 FEB 2018

Accepted 13 APR 2018

Accepted article online 19 APR 2018

Published online 13 MAY 2018

# Characteristics of the Mantle Flow System Beneath the Indochina Peninsula Revealed by Teleseismic Shear Wave Splitting Analysis

Youqiang Yu<sup>1</sup> , Stephen S. Gao<sup>2</sup> , Kelly H. Liu<sup>2</sup> , Ting Yang<sup>3</sup>, Mei Xue<sup>1</sup> , Khanh Phon Le<sup>4</sup>, and Jinyao Gao<sup>5</sup>

<sup>1</sup>State Key Laboratory of Marine Geology, Tongji University, Shanghai, China, <sup>2</sup>Geology and Geophysics Program, Missouri University of Science and Technology, Rolla, Missouri, USA, <sup>3</sup>School of Oceanography, Southern University of Science and Technology, Shenzhen, China, <sup>4</sup>Faculty of Oil and Gas, Hanoi University of Mining and Geology, Hanoi, Vietnam, <sup>5</sup>Second Institute of Oceanography, State Oceanic Administration, Hangzhou, China

**Abstract** Numerous geoscientific investigations have been conducted on the southeastern Tibetan Plateau and adjacent areas for understanding crustal and mantle deformation associated with the indentation of the Indian Plate into Eurasia. A number of key issues, such as the causes of a sudden change of fast polarization orientations from N-S to almost E-W at approximately 26°N revealed by shear wave splitting (SWS) studies, and the geodynamic implications of the transition still remain enigmatic, partially due to the lack of sufficient SWS measurements on the Indochina Peninsula. Here we employ the SWS technique to systematically illuminate upper mantle anisotropy beneath the Indochina Peninsula with an unprecedented data coverage. The resulting 409 SWS measurements from 29 stations show that upper mantle anisotropy beneath the vast majority of the study area is characterized by dominantly E-W fast orientations which are nearly orthogonal to the strike of most of the major tectonic features in the study area, ruling out significant lithospheric contributions to the observed anisotropy. This observation, when combined with results from seismic tomography, numerical modeling, surface movement, and focal mechanism investigations, suggests that the observed azimuthal anisotropy is mostly the consequence of absolute plate motion or the westward rollback of the oceanic Indian slab. The flow system induced by the rollback or absolute plate motion may experience regional alteration from mantle upwelling along the eastern edge of the slab and through a previously detected slab window, leading to local variations in the observed splitting parameters.

## 1. Introduction

Situated to the southeast of the eastern Himalayan syntaxis, the Indochina Peninsula (Figure 1) has mainly experienced two tectonic movements over the past 50 million years. The first is a clockwise rotation since 35 Ma as the result of the indentation of the Indian Plate into Eurasia, and the other is the subduction of the Indo-Burma Plate along its western margin (e.g., Huchon et al., 1994; Tapponnier et al., 1982). Tectonically, the Peninsula is mainly composed of the Indochina and Shan-Thai blocks, and is separated from the South China and Burma blocks by the Red River fault to the northeast and Sagaing fault to the northwest, respectively (Figure 1). The prominent Sagaing fault absorbs about 20 mm/yr of dextral motion induced by the highly oblique Indo-Burma convergence (Argus et al., 2011; Steckler et al., 2016). The initiation of the strike-slip faults probably started in the middle to late Eocene when the collision force between the Indian and Eurasian plates began to take effect. Extensive palaeomagnetic studies show that the Indochina Block has behaved as a rigid block since the Cretaceous and experienced clockwise rotations without significant internal deformation (e.g., Achache et al., 1983; Sato et al., 2007; Takemoto et al., 2009). Important constraints on past and current tectonic deformation can be obtained by exploring the patterns of seismic azimuthal anisotropy that they would generate (Silver & Chan, 1991).

Seismic azimuthal anisotropy reveals past and present deformation patterns in the crust and upper mantle, and is mainly attributed to lattice preferred orientation of intrinsically anisotropic crystals such as olivine (e.g., Silver, 1996; Silver & Chan, 1991; Zhang & Karato, 1995), and to shape preferred orientation of melt pockets or aligned cracks in the crust (e.g., Crampin, 1984) and mantle (Gao et al., 1997). Past tectonic

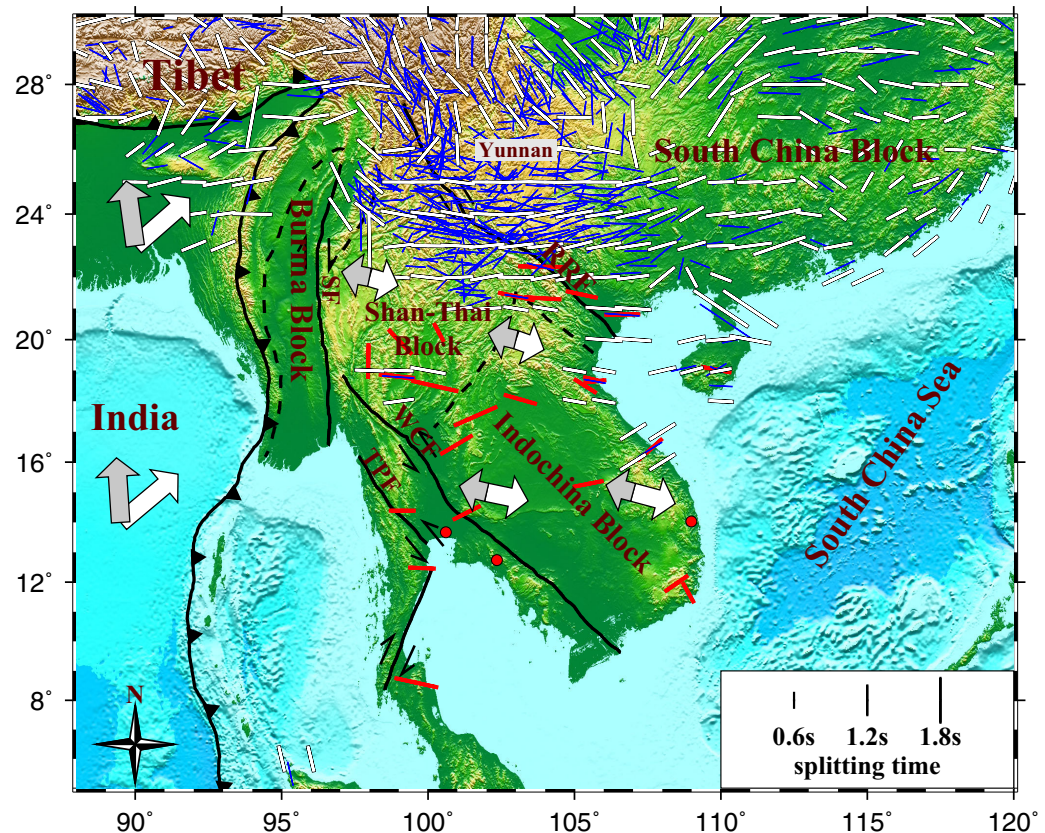


**Figure 1.** Shear wave splitting measurements of Southeast Asia. Red and blue bars indicate station-averaged SWS measurements from this and previous studies (Flesch et al., 2005; Huang et al., 2015a; Lev et al., 2006; Singh et al., 2006; Sol et al., 2007; Wang et al., 2008), respectively. White bars represent spatially averaged (in radius = 1° circles) SWS parameters from previous studies. Red dots indicate stations with all-null measurements, and white and gray arrows represent the absolute plate motion direction according to the NNR-MORVEL56 model (Argus et al., 2011) and the HS3-NUVEL-1A model (Gripp & Gordon, 2002), respectively. Black solid and dashed lines are major faults and sutures modified from Takemoto et al. (2009). RRF, Red River Fault; SF, Sagaing Fault; TPF, Three Pagodas Fault; and WCF, Wang Chao Fault.

processes can generate anisotropic fabrics preserved in the lithosphere as fossil anisotropy, and present-day progressive simple shear at the base of the lithosphere due to its movement relative to the underlain asthenosphere is another well-established mechanism for generating azimuthal anisotropy (Zhang & Karato, 1995). When propagating through a transversely isotropic medium with a horizontal axis of symmetry, a shear wave with a near vertical path of propagation would split into two (fast and slow) components with orthogonal polarization orientations. Such a phenomenon is called shear wave splitting (SWS). Azimuthal anisotropy is characterized by two splitting parameters, including the polarization orientation of the fast component ( $\phi$ ) and the delay time ( $\delta t$ ) between the fast and slow components.

SWS measurements in subduction zones reflect an integrated effect of anisotropy in the subslab mantle, slab, and mantle wedge with possible contributions from the overriding plate (Long & Wirth, 2013). A compilation of worldwide SWS measurements shows that the fast orientations vary with the distance to the trench (Long & Silver, 2008). Stations closer and farther to the trench are generally characterized as possessing trench-parallel and trench-perpendicular fast orientations, respectively. Complex patterns of fast orientations in some subduction areas were also observed (Long & Wirth, 2013). Azimuthal anisotropy observed above subducting slabs revealed from SWS measurements has been attributed to a series of factors such as slab pull, trench migration, effects of slab edges and morphology (Long & Wirth, 2013), as well as anisotropy originating from metastable olivine in the subducted slab (Liu et al., 2008). Possible existence of other olivine and/or serpentinite fabric types may also contribute to alter seismic anisotropy in the vicinity of subduction zones (Jung & Karato, 2001).

Previous SWS investigations in the areas affected by the Tibet-India collision have mostly focused on the Tibetan Plateau and the northern part of the Indochina Peninsula, while the central and southern Peninsula was sampled by a relatively limited number of stations (Figure 1). One of the most dramatic features of the splitting measurements in the region to the east and southeast of the Eastern syntaxis is a conspicuous change of the dominant fast orientations from approximately N-S in the area north of 26°N to E-W in the south (Figure 1; Flesch et al., 2005; Huang et al., 2015a; Lev et al., 2006; Sol et al., 2007; Wang et al., 2008). The nearly N-S fast orientations closely follow the surface tectonic fabrics and were interpreted as the result of vertically coherent lithospheric deformation (Flesch et al., 2005; Lev et al., 2006; Wang et al., 2008). However, the mechanisms responsible for the observed E-W fast orientations south of 26°N remain enigmatic. Proposed models include a transition from complete crust-mantle coupling at the north to complete decoupling at the south (Flesch et al., 2005; Sol et al., 2007; Xue et al., 2013), variations of lithospheric rheology (Lev et al., 2006), eastward asthenospheric flow from Tibet to eastern China (Bai et al., 2009; Huang et al., 2015a, 2015b), an eastward flow system induced by the subduction of the Indian Plate south of 26°N (Sol et al., 2007), and possibly westward rollback of the subducted Indian Plate (Lev et al., 2006; Sol et al., 2007).

In this study, we explore the upper mantle anisotropic structure and related mantle deformation beneath the Indochina Peninsula using the SWS technique with a spatial coverage that is more extensive than any of the previous regional-scale SWS studies (Bai et al., 2009; Xue et al., 2013), for the purpose of providing new constraints on various crustal and mantle deformation and circulation models.

## 2. Data and Method

The data set used for this study was recorded by 29 broadband seismic stations. Data from 19 stations were obtained from the Incorporated Research Institutions for Seismology (IRIS) Data Management Center (DMC). Five of the stations were operated by Tongji University over the period of 2009–2012 (Yang et al., 2015), and the other five were deployed in Vietnam by the University of Tokyo from early 2000 to late 2005 (Bai et al., 2009). In this study, three kinds of core refracted shear waves, including PKS, SKKS, and SKS (hereafter collectively called XKS), were utilized in the epicentral distance range of 120–180°, 95–180°, and 84–180° (Figure 2), respectively (Liu & Gao, 2013). The cutoff magnitude of the events is assigned as 5.6 for events with focal depths shallower than 100 km, and 5.5 for deeper events for the purpose of taking advantage of the sharper waveforms for deeper events. The true orientation of the N-S component determined by Yu et al. (2017a) was used to correct for station misorientation prior to the SWS analysis.

Splitting parameters were measured by following the set of procedures of Liu and Gao (2013), which was developed based on the minimization of transverse energy technique (Silver & Chan, 1991). The seismograms were initially windowed in the time period of 5 s before and 20 s after the predicted XKS arrival times, and then bandpass filtered using a Butterworth four-pole two-pass filter with corner frequencies of 0.04–0.5 Hz. All the SWS parameters were first automatically measured and ranked and then manually screened to verify the reliability in an interactive procedure. If necessary, the measuring parameters such as the beginning and end of the XKS time window, quality ranking, and filtering parameters, are manually adjusted (Liu & Gao, 2013; Yu et al., 2015).

The ranking of each SWS measurement was determined by considering such factors as the quality of the original and corrected seismograms, the remaining energy on the corrected transverse component, and the convergence and uniqueness of the optimal SWS parameters on the contour map of the transverse energy (Liu et al., 2008; Liu & Gao, 2013). The resulting splitting measurements were categorized as A (outstanding), B (good), C (poor), and N (null) based on the evaluation criteria of Liu and Gao (2013). A measurement is ranked as null

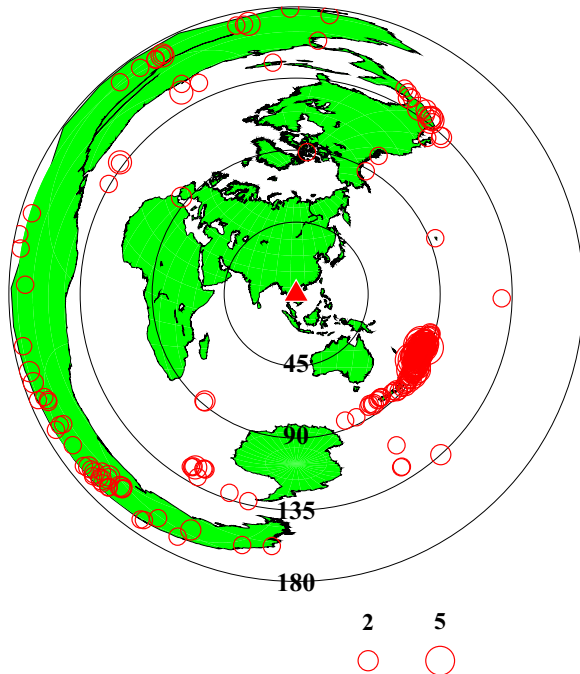


**Figure 2.** Spatial distribution of the 273 events used in this study (red circles). The size of the circles is proportional to the number of high-quality SWS measurements from each event. The red triangle represents the center of the study area.

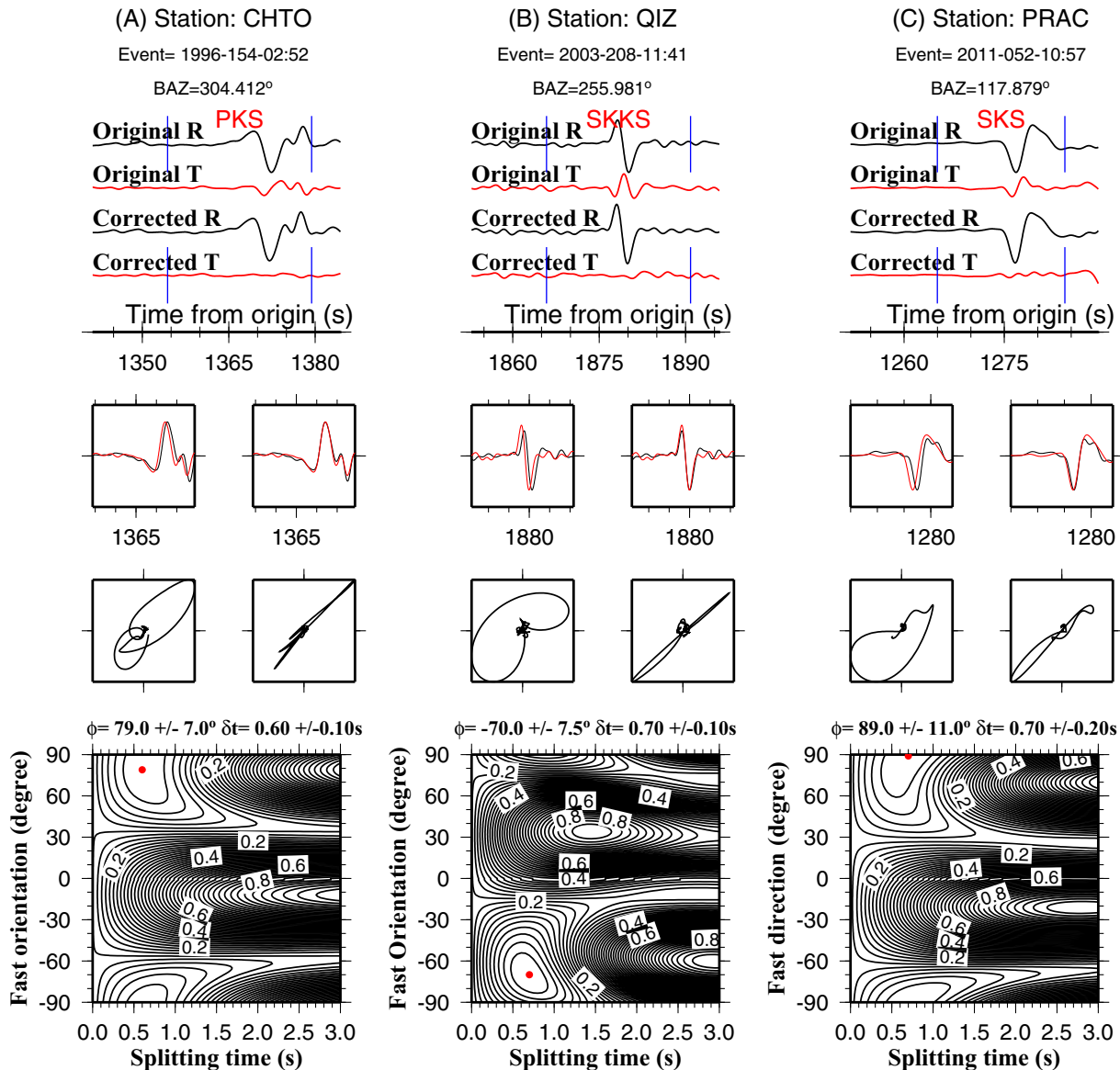


**Figure 3.** Examples of well-defined shear wave splitting measurements for each of the XKS phases (PKS, SKKS, and SKS) used in the study observed by three different stations. For each of the measurements, the top plot shows the original and corrected radial and transverse components, the middle plot shows the fast (red) and slow (black) components, and associated with the particle motion pattern (left) before and (right) after applying the optimal splitting time, and the bottom plot shows a contour map of transverse component energy as a function of candidate  $\phi$  and  $\delta t$ . The red dot on the contour map indicates the optimal splitting parameters.

when there is strong XKS energy on the original radial but no observable energy on the original transverse component. Figure 3 shows examples for the three XKS phases recorded at different stations. (Note that similar plots for all the measurements can be found at <http://web.mst.edu/%7Eyyqkc/Indochina-sws>.)

### 3. Results

A total of 409 pairs of Quality A or B SWS parameters were obtained from 273 events (Figure 2) recorded at 26 stations, including 40 PKS, 85 SKKS, and 284 SKS measurements, and no reliable A or B but only null measurements were obtained for the remaining three stations. The resulting spatial distributions of the station-averaged and individual measurements are shown in Figures 1 and 4, respectively. Details of the station-averaged and individual well-defined (Quality A and B) splitting parameters can be found in Table 1 and supporting information Table S1, respectively. In addition to the well-defined measurements, we also

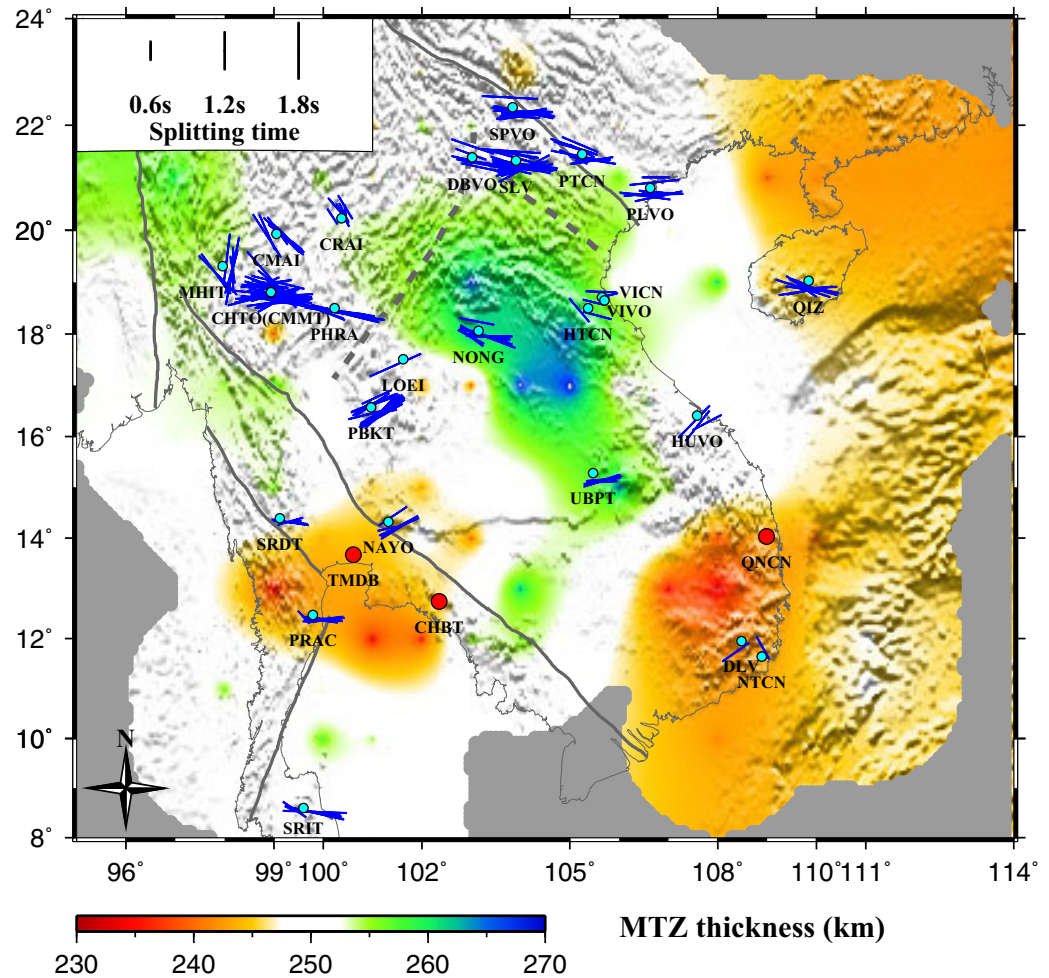


**Figure 4.** Individual splitting parameters plotted above the ray-piercing point at 110 km depth. Circles represent stations, and the red circles are stations with all-null measurements. The background image shows the thickness of the mantle transition zone (Yu et al., 2017b).

observed 213 null measurements (Figure 5), which are characterized by clear XKS arrivals on the radial component but unobservable energy on the original transverse component. They are the results of an absence of net azimuthal anisotropy along the XKS ray path from the core mantle boundary to the recording station, or reflect the situation when the back azimuth of the XKS event is parallel or perpendicular to the fast orientation (Liu & Gao, 2013; Silver & Chan, 1991).

The resulting fast orientations are dominantly E-W with a circular mean of  $93.5 \pm 23.2^\circ$ , which is statistically identical to the absolute plate motion (APM) direction of the Eurasian Plate ( $105^\circ$ ) calculated based on the NNR-MORVEL56 model (Argus et al., 2011). The simple mean of the splitting time is  $1.29 \pm 0.37$  s and is slightly larger than the global average of 1.0 s for continents (Silver, 1996). The thickness of the anisotropy layer is estimated to be  $144 \pm 41$  km if a 4% anisotropy is assumed (Silver & Chan, 1991). Regional variations are revealed in the Shan-Thai Block located at the NW part of the study area (Figures 1 and 4), where the fast orientations vary spatially from N-S or NW-SE in the north to E-W in the south. In the southernmost part of the Indochina Peninsula, only two well-defined SWS measurements were obtained, both have relatively small splitting times ( $0.90 \pm 0.14$  s), although data from a total of three stations are available in this area where Bai et al. (2009) and Xue et al. (2013) were unable to obtain reliable observations.

To investigate the existence of multilayered anisotropic structure which is characterized by systematic back-azimuthal variations of the splitting parameters with a period of  $90^\circ$  (Rumpker & Silver, 1998; Silver & Savage, 1994), we plot the individual splitting parameters against modulo- $90^\circ$  BAZ (Figures 6–8). The limited

**Table 1**  
*Station-Averaged SWS Measurements*

Station name	Lon. (°)	Lat. (°)	$\phi$ (°)	$\delta t$ (s)	No. of events
CHTO	98.940	18.810	95.5 ± 11.8	1.31 ± 0.03	148
CMAI	99.050	19.930	136.8 ± 8.3	1.24 ± 0.06	11
CMMT	98.940	18.810	99.2 ± 9.5	1.25 ± 0.07	27
CRAI	100.370	20.230	152.2 ± 11.1	0.71 ± 0.07	6
DBVO	103.020	21.390	101.9 ± 5.1	1.36 ± 0.12	8
DLV	108.480	11.950	55.0 ± 15.0	1.00 ± 0.33	1
HTCN	105.370	18.500	122.5 ± 18.1	0.93 ± 0.03	2
HUVO	107.580	16.410	47.9 ± 10.3	1.20 ± 0.12	3
LOEI	101.620	17.510	66.0 ± 3.5	1.75 ± 0.40	1
MHIT	97.960	19.310	0.8 ± 18.6	1.28 ± 0.13	12
NAYO	101.320	14.320	62.8 ± 6.6	1.10 ± 0.12	6
NONG	103.150	18.060	106.0 ± 11.1	1.23 ± 0.09	12
NTCN	108.890	11.640	151.0 ± 17.0	0.80 ± 0.25	1
PBKT	100.970	16.570	59.1 ± 8.1	1.35 ± 0.04	28
PHRA	100.230	18.500	102.8 ± 4.1	1.78 ± 0.12	13
PLVO	106.630	20.810	89.2 ± 5.8	1.29 ± 0.09	9
PRAC	99.790	12.470	92.4 ± 13.1	0.96 ± 0.06	13
PTCN	105.250	21.450	102.2 ± 11.9	1.17 ± 0.06	14
QIZ	109.840	19.030	100.9 ± 14.9	1.10 ± 0.10	12
SLV	103.910	21.330	93.5 ± 9.5	1.35 ± 0.05	50
SPVO	103.840	22.340	90.7 ± 7.5	1.65 ± 0.07	13
SRDT	99.120	14.390	90.1 ± 9.4	0.93 ± 0.09	5
SRIT	99.600	8.600	102.4 ± 10.2	1.65 ± 0.17	6
UBPT	105.470	15.280	79.0 ± 6.1	1.10 ± 0.05	5
VICN	105.650	18.710	104.0 ± 10.5	0.70 ± 0.15	1
VIVO	105.700	18.650	84.0 ± 8.1	0.77 ± 0.17	2

BAZ range for most of the stations prevents a reliable determination of the existence or absence of complex anisotropy, although in general, the measurements from events with different back azimuths are quite consistent. For stations MHIT and CHTO (Figure 8), the splitting parameters vary slightly as functions of the ray-piercing point location (Liu & Gao, 2013). In the absence of clear periodic back-azimuthal variations of the individual splitting parameters, in the following, we assume that a single transversely isotropic layer with a horizontal axis of symmetry is responsible for the splitting measurements.

## 4. Discussion

### 4.1. Relationships With Lithospheric Fabrics and APM

Vertically coherent lithospheric deformation can lead to the development of lithospheric anisotropy with fast orientations parallel to the strike of lithospheric fabrics, possibly attributed to mineralogical alignment in response to regional shortening or extension (Silver, 1996; Silver & Chan, 1991). The predominantly E-W fast orientations observed at the majority of the stations are significantly different from the strike of regional tectonic features (Figure 1) such as the well-developed strike-slip Red River and Wang Chao faults (mostly in the SE-NW direction). In addition, if lithospheric fabrics are the main source of the observed azimuthal anisotropy, the splitting times are expected to increase near the shear zones, where lithospheric deformation and strain localization are the most intensive. This correspondence is not revealed from the resulting SWS measurements (Figures 4 and 9), suggesting limited contributions from lithospheric fabrics.

The relative movement between the lithosphere and asthenosphere can induce simple shear strain, which would align mantle olivine and form APM-parallel fast orientations (Liu et al., 2014; Zhang & Karato, 1995), but only when the asthenosphere is stationary or moving at the opposite or same direction (with a different rate) relative to the plate. The HS3-NUVEL-1A model (Gripp & Gordon, 2002) developed under the assumption of a fixed Pacific hot spot reference frame indicates that the Indochina Peninsula is moving toward the WNW direction (about  $-77^\circ$  measured clockwise from the north) at a rate of 23 mm/yr. In comparison, a no-net rotation APM model, NNR-MORVEL56 (Argus et al., 2011), predicts a speed of about 30 mm/yr and

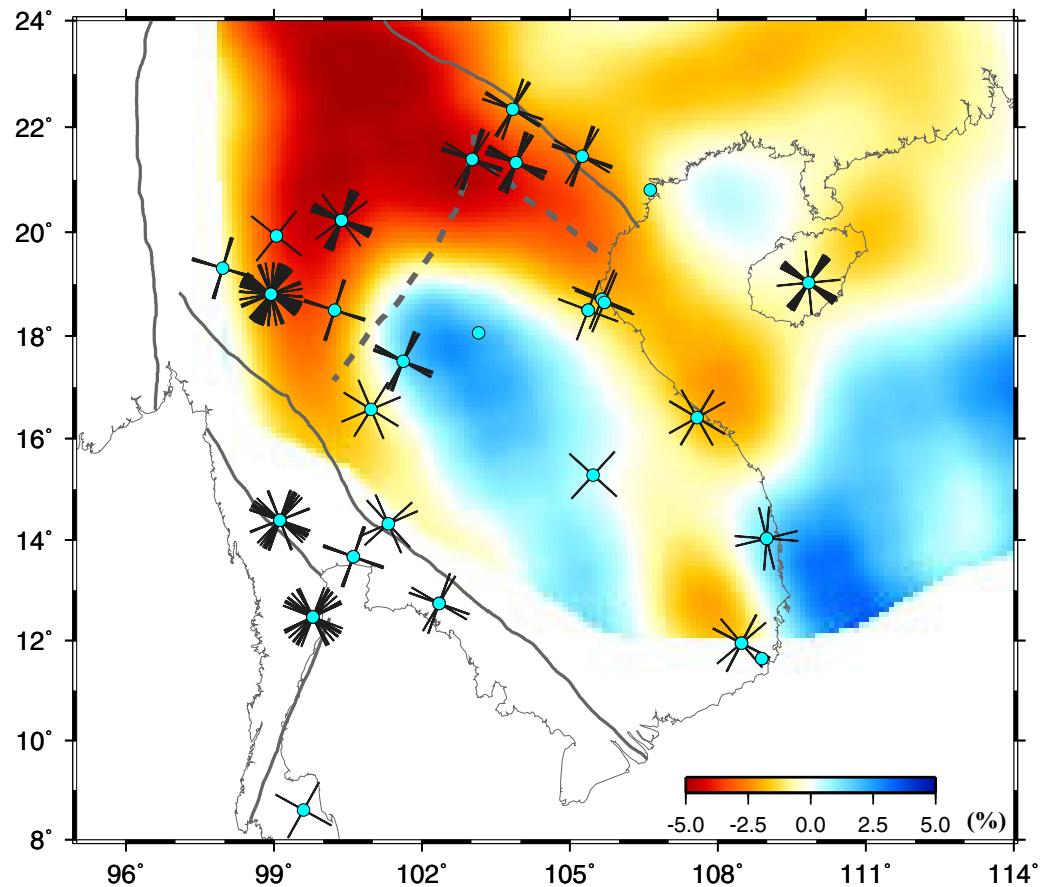


**Figure 5.** Observed null measurements from this study (black bars) plotted on top of S wave velocity anomalies at 110 km depth (Yang et al., 2015). For each null measurement, two bars are plotted at the station, with orientations being parallel and perpendicular to the back azimuth of the event, respectively.

an almost opposite direction ( $105^\circ$ ). Despite the difference in the predicted directions from the APM models, the orientation of the APM from both HS3-NUVEL-1A and NNR-MORVEL56 models approximately parallels to the observed fast orientations in most regions of the Peninsula, except for the southernmost one-third of the Peninsula and beneath the three stations located at the northwestern corner of the study area (Figure 1).

Previous SWS studies (e.g., Huang et al., 2011; Liu et al., 2008) suggested that the fast orientations observed at most of the stations in mainland China are consistent with predictions from the HS3-NUVEL-1A model. One of the areas showing significant discrepancies between the two is southeastern Tibetan Plateau, where the fast orientations and the APM are almost perpendicular to each other. The N-S oriented anisotropy in the area is attributable to either vertically coherent lithospheric deformation (e.g., Flesch et al., 2005; Wang et al., 2008) or southeast or south directed asthenospheric flow in response to the northward indentation of the Indian lithosphere (Bai et al., 2009; Huang et al., 2015a, 2015b), among other proposed mechanisms. Under these hypotheses, anisotropy produced by lithospheric deformation or mantle flow beneath southeastern Tibetan Plateau must be strong enough to overprint anisotropy produced by the APM.

If we assume that the E-W fast orientations observed on the Indochina Peninsula are APM-related, the spatial distribution of the observations has several important geodynamic implications. First, vertically coherent lithospheric deformation related to the continental collision has insignificant effects on the Peninsula. This is consistent with the low topography and lack of shallow earthquakes in the interior of the Peninsula. Second, south and southeast directed mantle flow system related to the collision terminates at about  $26^\circ\text{N}$ , and may turn eastward at this latitude (Figure 1). Third, as detailed below, upwelling flow beneath the southern part of the Peninsula might be responsible for reducing the strength of APM-related flow.

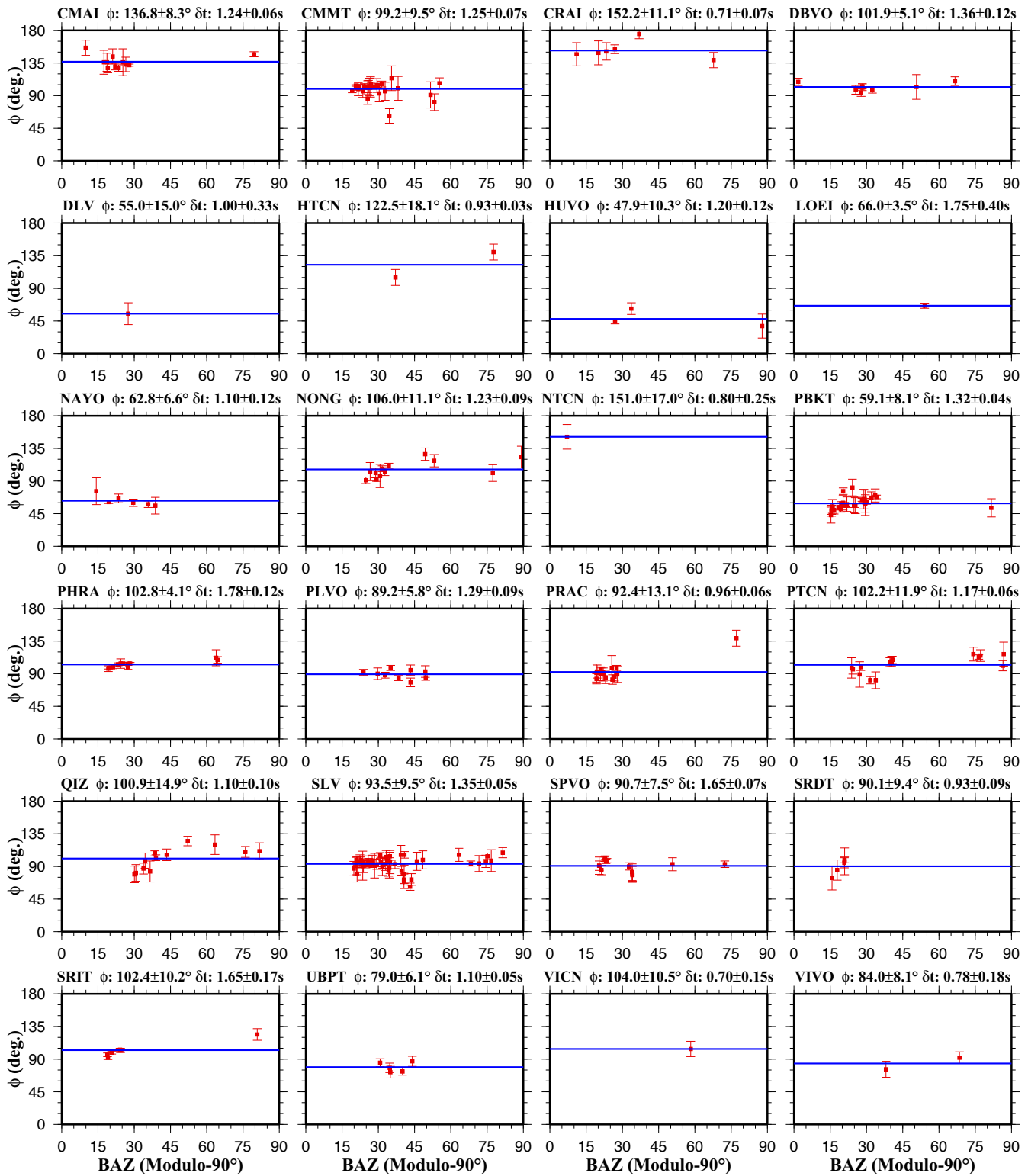


Figure 6. Fast orientations plotted against modulo-90° back azimuth for each station. The blue lines indicate the station-averaged values.

#### 4.2. Mantle Flow Induced by Slab Subduction and Rollback

Another possible cause of the dominantly E-W fast orientations observed on the Peninsula is a corner flow system induced by the eastward subduction of the Indian Plate, an anisotropy-forming mechanism that is frequently proposed for SWS measurements above mantle wedges (e.g., Long & Silver, 2008; Long & Wirth, 2013).

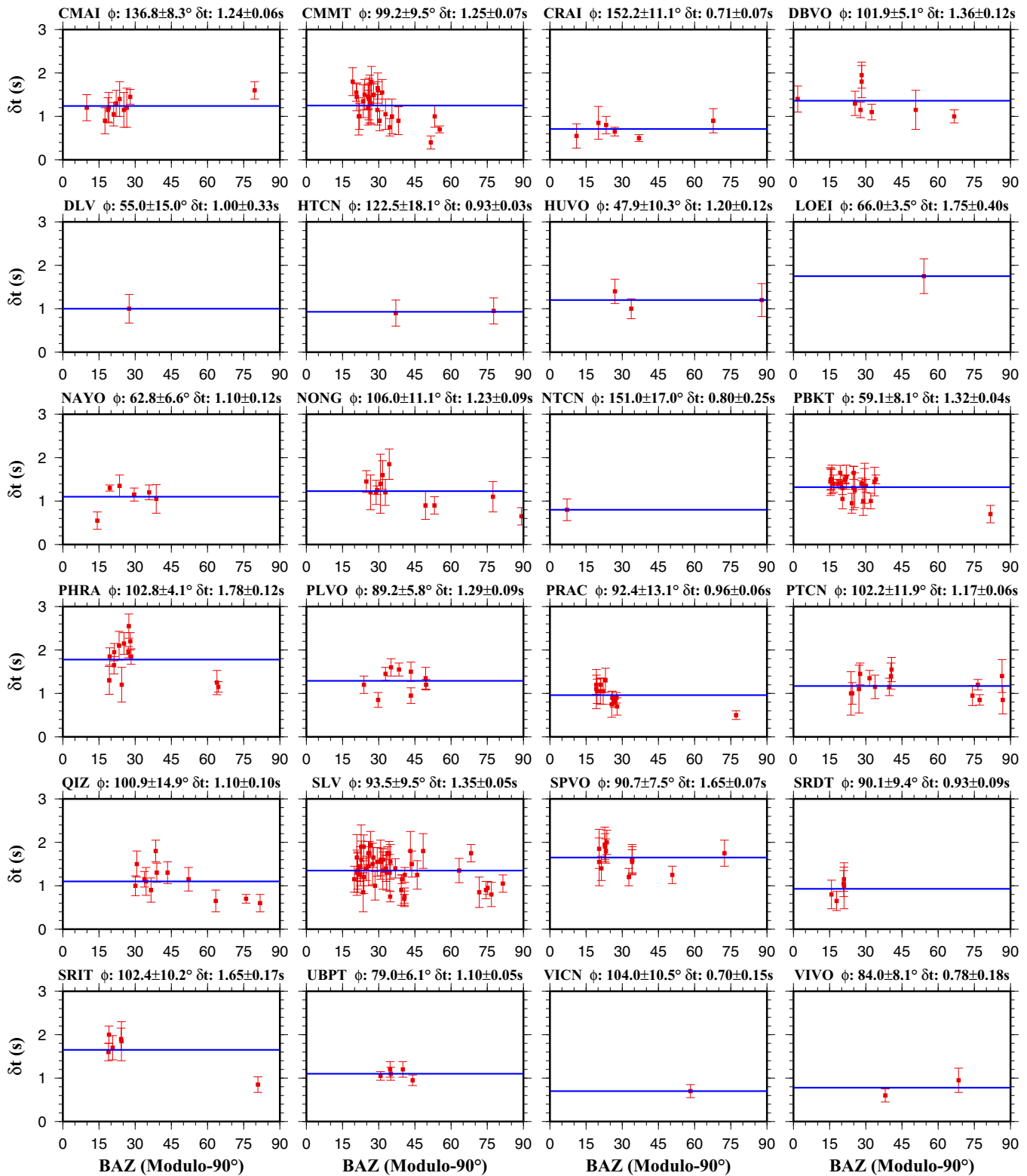
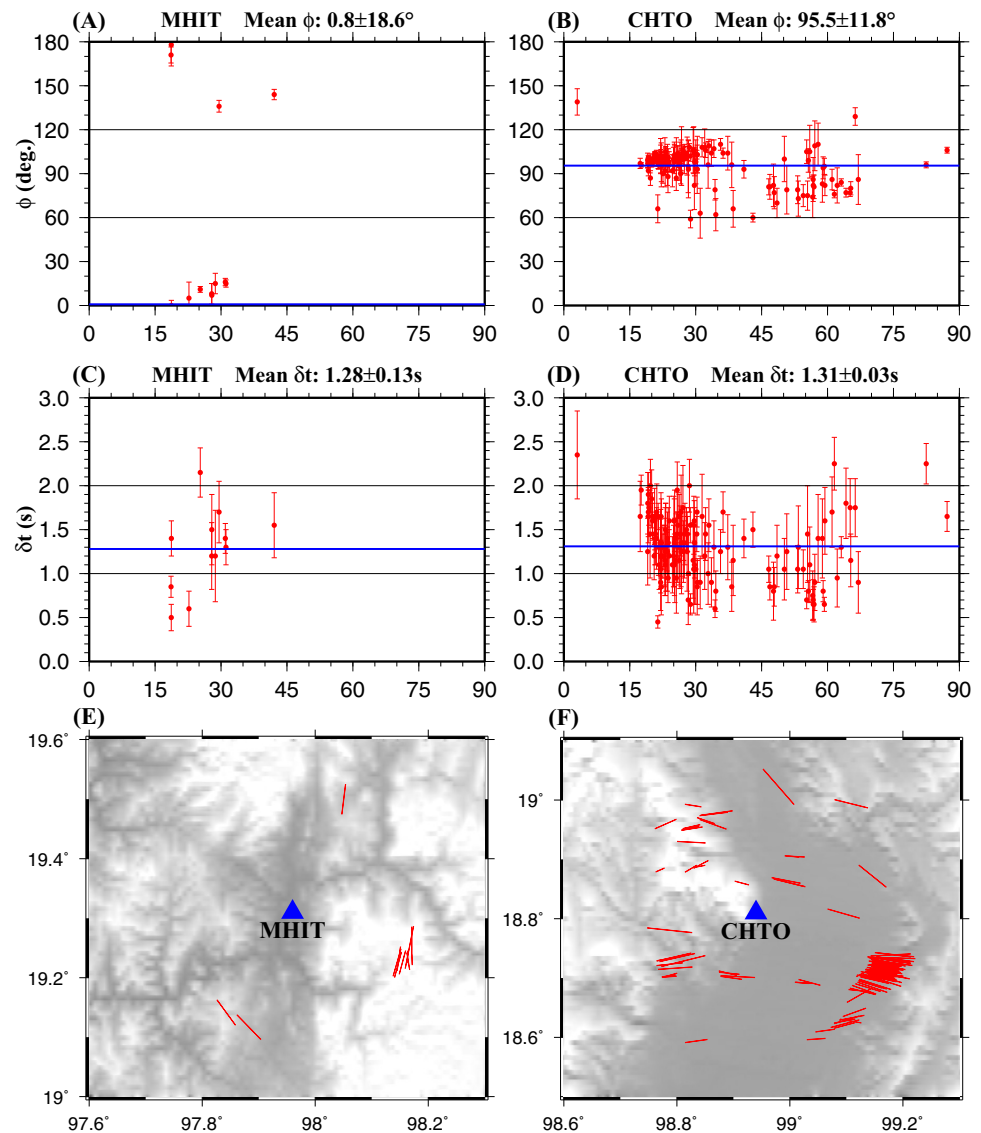


Figure 7. Same as Figure 6 but for splitting times.

While seismic tomography (e.g., Bijwaard et al., 1998; Li et al., 2008; Pesicek et al., 2008) and receiver function studies (Yu et al., 2017b) have demonstrated that the Indian slab has reached the mantle transition zone (MTZ), the key issue of whether the subduction is still active remains debated. A recent focal



**Figure 8.** SWS measurements for stations (left plots) MHIT and (right plots) CHTO. (a and b) Fast orientations plotted against modulo-90° back azimuth; (c and d) same as Figures 8a and 8b but for splitting times; (e and f) SWS parameters plotted above ray-piercing points at 110 km depth on a topographic map and the blue triangles display the station locations.

mechanism study reveals that the *P* axis of earthquakes in the Benioff zone beneath the Burma Block has a predominantly NNE direction, which is similar to the direction of relative plate motion between the Indian and Eurasian plates, and argues against active subduction (Rao & Kumar, 1999). In addition, the intermediate-depth earthquakes under the accretionary wedge of the Indo-Burmese arc are characterized as intraslab type instead of occurring at the contact surface between the wedge and the subducted slab (Kundu & Gahalaut, 2012), probably as the result of reactivation of the preserved geological fabrics within the slab (Gahalaut et al., 2013).

Under the assumption that the subduction is inactive, slab rollback is an alternative mechanism responsible for the observed E-W fast orientations, besides APM-related simple shear strain (Figure 10). It has been suggested that slab rollback can initiate subhorizontal mantle return flow and generate tectonically significant shear stresses at the base of the overriding plate (Chen et al., 2016), leading to trench-orthogonal fast orientations. Beneath the Indochina Peninsula, three-dimensional thermomechanical modeling indicates that mantle flow due to slab rollback plays the dominant role in modulating the surface strain and kinematics (Sternai et al., 2014).

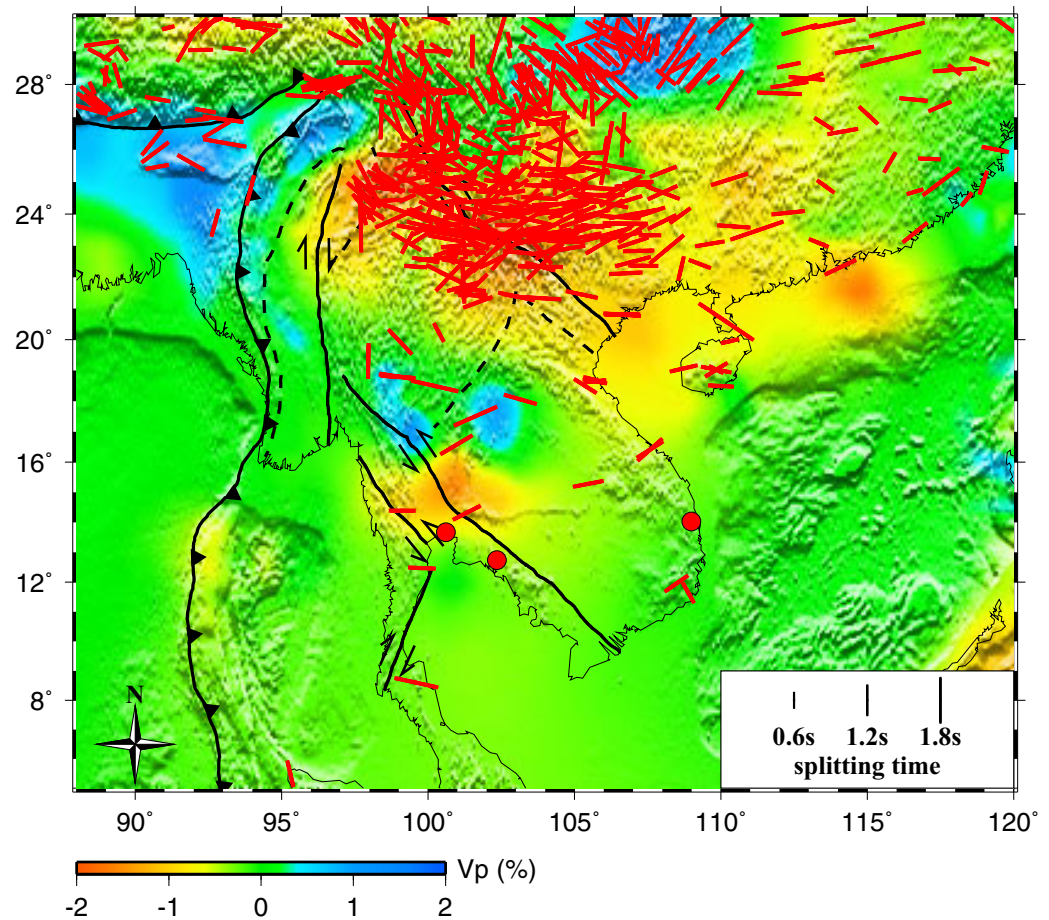


**Figure 9.** Station-averaged SWS measurements from this and previous studies (red bars) plotted on top of *P* wave velocity anomalies at 110 km depth (Li et al., 2008). Red dots indicate stations with all-null measurements from this study.

The toroidal component of the mantle flow system (Faccenna et al., 2010; Singh et al., 2006; Sternai et al., 2014) can explain the N-S or SE-NW fast orientations observed at the three stations located at the NW edge of the study area (Figure 10), although other mechanisms such as strong lithospheric contributions cannot be ruled out due to limited spatial coverage by the seismic stations. Another possible cause of the SE-NW fast orientations observed at the three stations is the presence of other olivine fabric types (besides the A-type), especially the B-type, which develops under low temperature conditions in a subduction system and can produce fast orientations that tend to be orthogonal to the flow direction (Jung et al., 2006; Long & Silver, 2008).

#### 4.3. Mantle Upwelling Beneath the Southern Indochina Peninsula

One of the possible causes of the weak and spatially varying anisotropy observed beneath the southern part of the Peninsula (Figure 1) may be mantle upwelling along the eastern edge of the subducted slab and through a slab window (Figure 10). The location of the eastern edge of the subducted plate and the presence of a slab window have been revealed by seismic tomography and receiver function studies (Li et al., 2008; Pesicek et al., 2008; Yu et al., 2017b). The upwelling flow is also suggested from geodynamic modeling (Faccenna et al., 2010) and geochemical (Hoang & Flower, 1998) studies, and is thought to be responsible for the low seismic velocity anomalies in the upper mantle (e.g., Huang et al., 2015b; Pesicek et al., 2008; Yang et al., 2015). It might also be the cause of the thinner than normal MTZ thickness (Yu et al., 2017b; Figure 4), which is an indicator of higher than normal temperature.

Subvertical shear strain near the center of the mantle upwelling may result in weak or negligible anisotropy, with spatially varying fast orientations (Walker et al., 2001). As demonstrated in Figure 4, the spatial correspondence between the characteristics of the splitting measurements and the thickness of the mantle

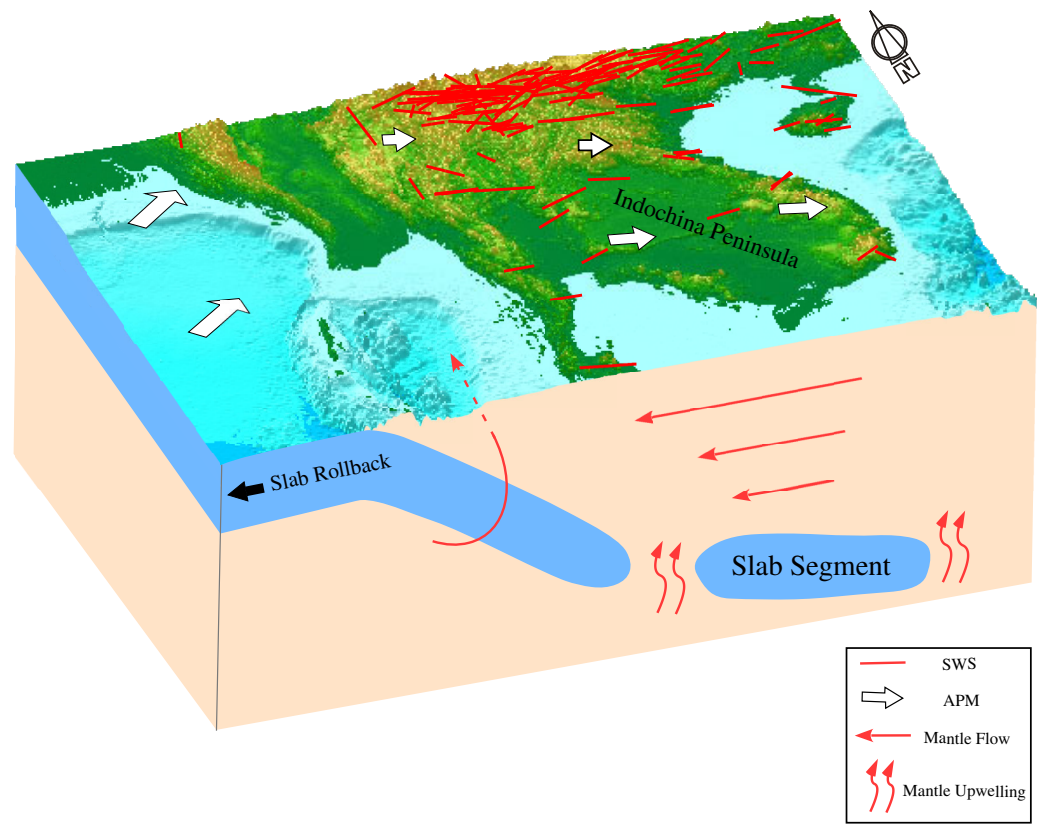


**Figure 10.** A schematic cartoon showing the formation mechanisms of the observed seismic anisotropy beneath the Indochina Peninsula generated based on our observations and previous studies (Li et al., 2008; Pesicek et al., 2008; Yu et al., 2017b).

transition zone is remarkable, as all the three stations with all-null measurements and the two stations with splitting parameters that are inconsistent with those found at the majority of the stations are located in areas underlain by an MTZ that is 5 or more kilometers thinner than the global average of 250 km. We would like to emphasize that due to the limited station coverage and lack of high resolution seismic tomography images, the existence of the mantle upwelling and thus the causes of the azimuthal anisotropy beneath the southern part of the Peninsula remain speculative. Additional observational and geodynamic modeling studies are required in order to pinpoint the mantle deformation field beneath this part of the study area and to provide robust explanations for the observed azimuthal anisotropy.

#### Acknowledgments

Seismic waveform data from 19 of the 29 stations are publicly available at the IRIS DMC (lasted accessed: November, 2017), and data in SAC (Seismic Analysis Codes) format for the remaining stations can be accessed from <http://web.mst.edu/%7Eyyqkc/Indochina-sws>. We thank two anonymous reviewers for their constructive comments. This work is supported by the National Natural Science Foundation of China (grants 41606043 and 41676033), the National Program on Global Change and Air-Sea Interaction (grant GASI-GEOGE-05), and the Fundamental Research Funds for the Central Universities (grant kx0135020171801), and the United States National Science Foundation (grant 0911346).

#### 5. Conclusions

XKS splitting measurements with an unprecedented spatial coverage indicate that the E-W fast orientations previously observed in the northern Indochina Peninsula extend to the whole Peninsula. The mostly N-S oriented mantle anisotropy observed on SE Tibetan Plateau is limited to about 26°N, in spite of the fact that N-S directed crustal structures extend further south into the Peninsula, beneath which mantle flow induced by APM or the westward rollback of the subducted Indian Plate becomes the dominant mechanism in generating the mostly E-W fast orientations. Upwelling of mantle flow beneath the southern part of the Peninsula might be responsible for the spatially varying fast orientations and weak anisotropy.

#### References

- Achache, J., Courtillot, V., & Besse, J. (1983). Paleomagnetic constraints on the late Cretaceous and Cenozoic tectonics of southeastern Asia. *Earth and Planetary Science Letters*, 63(1), 123–136. [https://doi.org/10.1016/0012-821X\(83\)90028-6](https://doi.org/10.1016/0012-821X(83)90028-6)
- Argus, D. F., Gordon, R. G., & DeMets, C. (2011). Geologically current motion of 56 plates relative to the no-net-rotation reference frame. *Geochemistry, Geophysics, Geosystems*, 12, Q11001. <https://doi.org/10.1029/2011GC003751>

- Bai, L., Lidaka, T., Kawakatsu, H., Morita, Y., & Dzung, N. Q. (2009). Upper mantle anisotropy beneath Indochina block and adjacent regions from shear-wave splitting analysis of Vietnam broadband seismograph array data. *Physics of the Earth and Planetary Interiors*, 176(1–2), 33–43. <https://doi.org/10.1016/j.pepi.2009.03.008>
- Bijwaard, H., Spakman, W., & Engdahl, E. R. (1998). Closing the gap between regional and global travel time tomography. *Journal of Geophysical Research*, 103(B12), 30055–30078. <https://doi.org/10.1029/98JB02467>
- Chen, Z., Schellart, W. P., Strak, V., & Duarte, J. C. (2016). Does subduction-induced mantle flow drive backarc extension? *Earth and Planetary Science Letters*, 441, 200–210. <https://doi.org/10.1016/j.epsl.2016.02.027>
- Crampin, S. (1984). Effective anisotropic elastic constants for wave propagation through cracked solids. *Geophysical Journal International*, 76(1), 135–145. <https://doi.org/10.1111/j.1365-246X.1984.tb05029.x>
- Faccenna, C., Becker, T. W., Lallemand, S., Lagabrielle, Y., Funicello, F., & Piromallo, C. (2010). Subduction-triggered magmatic pulses: A new class of plumes? *Earth and Planetary Science Letters*, 299(1–2), 54–68. <https://doi.org/10.1016/j.epsl.2010.08.012>
- Flesch, L. M., Holt, W. E., Silver, P. G., Stephenson, M., Wang, C. Y., & Chan, W. W. (2005). Constraining the extent of crust-mantle coupling in central Asia using GPS, geologic, and shear wave splitting data. *Earth and Planetary Science Letters*, 238(1–2), 248–268. <https://doi.org/10.1016/j.epsl.2005.06.023>
- Gahalaut, V. K., Kundu, B., Laishram, S. S., Catherine, J., Kumar, A., Singh, M. D., et al. (2013). Aseismic plate boundary in the Indo-Burmese wedge, northwest Sunda Arc. *Geology*, 41(2), 235–238. <https://doi.org/10.1130/G33771.1>
- Gao, S., Davis, P. M., Liu, H., Slack, P. D., Rigor, A. W., Zorin, Y. A., et al. (1997). SKS splitting beneath continental rift zones. *Journal of Geophysical Research*, 102(B10), 22781–22797. <https://doi.org/10.1029/97JB01858>
- Gripp, A. E., & Gordon, R. G. (2002). Young tracks of hotspots and current plate velocities. *Geophysical Journal International*, 150(2), 321–361. <https://doi.org/10.1046/j.1365-246X.2002.01627.x>
- Hoang, N., & Flower, M. (1998). Petrogenesis of Cenozoic basalts from Vietnam: Implications for origin of a diffuse igneous province. *Journal of Petrology*, 39(3), 369–395. <https://doi.org/10.1093/ptro/39.3.369>
- Huang, Z., Wang, L., Xu, M., Ding, Z., Wu, Y., Wang, P., et al. (2015a). Teleseismic shear-wave splitting in SE Tibet: Insight into complex crust and upper-mantle deformation. *Earth and Planetary Science Letters*, 432, 354–362. <https://doi.org/10.1016/j.epsl.2015.10.027>
- Huang, Z., Zhao, D., & Wang, L. (2015b). P wave tomography and anisotropy beneath Southeast Asia: Insight into mantle dynamics. *Journal of Geophysical Research*, 120, 5154–5174. <https://doi.org/10.1002/2015JB012098>
- Huang, Z., Wang, L., Zhao, D., Mi, N., & Xu, M. (2011). Seismic anisotropy and mantle dynamics beneath China. *Earth and Planetary Science Letters*, 306(1–2), 105–117. <https://doi.org/10.1016/j.epsl.2011.03.038>
- Huchon, P., Le Pichon, X., & Rangin, C. (1994). Indochina Peninsula and the collision of India and Eurasia. *Geology*, 22(1), 27–30. [https://doi.org/10.1130/0091-7613\(1994\)022<0027:IPATCO>2.3.CO;2](https://doi.org/10.1130/0091-7613(1994)022<0027:IPATCO>2.3.CO;2)
- Jung, H., & Karato, S. I. (2001). Water-induced fabric transitions in olivine. *Science*, 293(5534), 1460–1463. <https://doi.org/10.1126/science.1062235>
- Jung, H., Katayama, I., Jiang, Z., Hiraga, T., & Karato, S. I. (2006). Effect of water and stress on the lattice-preferred orientation of olivine. *Tectonophysics*, 421(1–2), 1–22. <https://doi.org/10.1016/j.tecto.2006.02.011>
- Kundu, B., & Gahalaut, V. K. (2012). Earthquake occurrence processes in the Indo-Burmese wedge and Sagaing fault region. *Tectonophysics*, 524–525, 135–146. <https://doi.org/10.1016/j.tecto.2011.12.031>
- Lev, E., Long, M. D., & van der Hilst, R. D. (2006). Seismic anisotropy in Eastern Tibet from shear wave splitting reveals changes in lithospheric deformation. *Earth and Planetary Science Letters*, 251(3–4), 293–304. <https://doi.org/10.1016/j.epsl.2006.09.018>
- Li, C., van der Hilst, R., Meltzer, A. S., & Engdahl, E. R. (2008). Subduction of the Indian lithosphere beneath the Tibetan Plateau and Burma. *Earth and Planetary Science Letters*, 274(1–2), 157–168. <https://doi.org/10.1016/j.epsl.2008.07.016>
- Liu, K. H., Elsheikh, A., Lemnifi, A., Purevsuren, U., Ray, M., Refayee, H., et al. (2014). A uniform database of teleseismic shear wave splitting measurements for the western and central United States. *Geochemistry, Geophysics, Geosystems*, 15, 2075–2085. <https://doi.org/10.1002/2014GC005267>
- Liu, K. H., & Gao, S. S. (2013). Making reliable shear-wave splitting measurements. *Bulletin of the Seismological Society of America*, 103(5), 2680–2693. <https://doi.org/10.1785/0120120355>
- Liu, K. H., Gao, S. S., Gao, Y., & Wu, J. (2008). Shear wave splitting and mantle flow associated with the deflected Pacific slab beneath north-east Asia. *Journal of Geophysical Research*, 113, B01305. <https://doi.org/10.1029/2007JB005178>
- Long, M. D., & Silver, P. G. (2008). The subduction zone flow field from seismic anisotropy: A global view. *Science*, 319(5861), 315–318. <https://doi.org/10.1126/science.1150809>
- Long, M. D., & Wirth, E. A. (2013). Mantle flow in subduction systems: The mantle wedge flow field and implications for wedge processes. *Journal of Geophysical Research*, 118(2), 583–606. <https://doi.org/10.1002/jgrb.50063>
- Pesicek, J. D., Thurber, C. H., Widiyantoro, S., Engdahl, E. R., & DeShon, H. R. (2008). Complex slab subduction beneath northern Sumatra. *Geophysical Research Letters*, 35, L20303. <https://doi.org/10.1029/2008GL035262>
- Rao, N. P., & Kumar, M. R. (1999). Evidences for cessation of Indian plate subduction in the Burmese arc region. *Geophysical Research Letters*, 26(20), 3149–3152. <https://doi.org/10.1029/1999GL005396>
- Rumpker, G., & Silver, P. G. (1998). Apparent shear-wave splitting parameters in the presence of vertically varying anisotropy. *Geophysical Journal International*, 135(3), 790–800. <https://doi.org/10.1046/j.1365-246X.1998.00660.x>
- Sato, K., Liu, Y., Wang, Y., Yokoyama, M., Yoshioka, S. Y., Yang, Z., et al. (2007). Paleomagnetic study of Cretaceous rocks from Pu'er, western Yunnan, China: Evidence of internal deformation of the Indochina block. *Earth and Planetary Science Letters*, 258(1–2), 1–15. <https://doi.org/10.1016/j.epsl.2007.02.043>
- Silver, P. G. (1996). Seismic anisotropy beneath the continents: Probing the depths of geology. *Annual Review of Earth and Planetary Sciences*, 24(1), 385–432. <https://doi.org/10.1146/annurev.earth.24.1.385>
- Silver, P. G., & Chan, W. W. (1991). Shear wave splitting and subcontinental mantle deformation. *Journal of Geophysical Research*, 96(B10), 16429–16454. <https://doi.org/10.1029/91JB00899>
- Silver, P. G., & Savage, M. K. (1994). The interpretation of shear-wave splitting parameters in the presence of two anisotropic layers. *Geophysical Journal International*, 119(3), 949–963. <https://doi.org/10.1111/j.1365-246X.1994.tb04027.x>
- Singh, A., Kumar, M. R., Raju, P. S., & Ramesh, D. S. (2006). Shear wave anisotropy of the northeast Indian lithosphere. *Geophysical Research Letters*, 33, L16302. <https://doi.org/10.1029/2006GL026106>
- Sol, S., Meltzer, A., Bürgmann, R., van der Hilst, R. D., King, R., Chen, Z., et al. (2007). Geodynamics of the southeastern Tibetan Plateau from seismic anisotropy and geodesy. *Geology*, 35(6), 563–566. <https://doi.org/10.1130/G23408A.1>
- Steckler, M. S., Mondal, D. R., Akhter, S. H., Seeber, L., Feng, L., Gale, J., et al. (2016). Locked and loading megathrust linked to active subduction beneath the Indo-Burman Ranges. *Nature Geoscience*, 9(8), 615–618. <https://doi.org/10.1038/ngeo2760>

- Sternai, P., Jolivet, L., Menant, A., & Gerya, T. (2014). Driving the upper plate surface deformation by slab rollback and mantle flow. *Earth and Planetary Science Letters*, *405*, 110–118. <https://doi.org/10.1016/j.epsl.2014.08.023>
- Takemoto, K., Sato, S., Chanthavichith, K., Inthavong, T., Inokuchi, H., Fujihara, M., et al. (2009). Tectonic deformation of the Indochina Peninsula recorded in the Mesozoic palaeomagnetic results. *Geophysical Journal International*, *179*(1), 97–111. <https://doi.org/10.1111/j.1365-246X.2009.04274.x>
- Tapponnier, P., Peltzer, G., Le Dain, A. Y., Armijo, R., & Cobbold, P. (1982). Propagating extrusion tectonics in Asia: New insights from simple experiments with plasticine. *Geology*, *10*(12), 611–616. [https://doi.org/10.1130/0091-7613\(1982\)10<611:PETIAN>2.0.CO;2](https://doi.org/10.1130/0091-7613(1982)10<611:PETIAN>2.0.CO;2)
- Walker, K. T., Bokelmann, G. H. R., & Klemperer, S. L. (2001). Shear-wave splitting to test mantle deformation models around Hawaii. *Geophysical Research Letters*, *28*(22), 4319–4322.
- Wang, C. Y., Flesch, L. M., Silver, P. G., Chang, L. J., & Chan, W. W. (2008). Evidence for mechanically coupled lithosphere in central Asia and resulting implications. *Geology*, *36*(5), 363–366. <https://doi.org/10.1130/G24450A.1>
- Xue, M., Le, K. P., & Yang, T. (2013). Seismic anisotropy surrounding South China Sea and its geodynamic implications. *Marine Geophysical Research*, *34*(3–4), 407–429. <https://doi.org/10.1007/s11001-013-9194-4>
- Yang, T., Liu, F., Harmon, N., Le, K. P., Gu, S., & Xue, M. (2015). Lithospheric structure beneath Indochina block from Rayleigh wave phase velocity tomography. *Geophysical Journal International*, *200*(3), 1582–1595. <https://doi.org/10.1093/gji/ggu488>
- Yu, Y., Hung, T. D., Yang, T., Xue, M., Liu, K. H., & Gao, S. S. (2017a). Lateral variations of crustal structure beneath the Indochina Peninsula. *Tectonophysics*, *712–713*, 193–199. <https://doi.org/10.1016/j.tecto.2017.05.023>
- Yu, Y., Gao, S. S., Liu, K. H., Yang, T., Xue, M., & Le, K. P. (2017b). Mantle transition zone discontinuities beneath the Indochina Peninsula: Implications for slab subduction and mantle upwelling. *Geophysical Research Letters*, *44*, 7159–7167. <https://doi.org/10.1002/2017GL073528>
- Yu, Y., Gao, S. S., Moidaki, M., Reed, C. A., & Liu, K. H. (2015). Seismic anisotropy beneath the incipient Okavango rift: Implications for rifting initiation. *Earth and Planetary Science Letters*, *430*, 1–8. <https://doi.org/10.1016/j.epsl.2015.08.009>
- Zhang, S., & Karato, S. I. (1995). Lattice preferred orientation of olivine aggregates deformed in simple shear. *Nature*, *375*(6534), 774–777. <https://doi.org/10.1038/375774a0>